Pentamidine sensitizes Gram-negative pathogens to antibiotics and overcomes acquired colistin resistance

Jonathan M. Stokes[1], Craig R. MacNair[1], Bushra Ilyas[1], Shawn French[1], Jean-Philippe Côté[1], Catrien Bouwman[2], Maya A. Farha[1], Arthur O. Sieron[1], Chris Whitfield[2], Brian K. Coombes[1], and Eric D. Brown[1]*

[1]Michael G. DeGroote Institute for Infectious Disease Research, Department of Biochemistry and Biomedical Sciences, McMaster University, Hamilton, Ontario, Canada, L8N 3Z5
[2]Department of Molecular and Cellular Biology, University of Guelph, Guelph, Ontario, Canada, N1G 2W1

*Correspondence: ebrown@mcmaster.ca

This file contains:

Supplementary Figures 1-7

Additional supplementary information:

Supplementary Tables 1-6

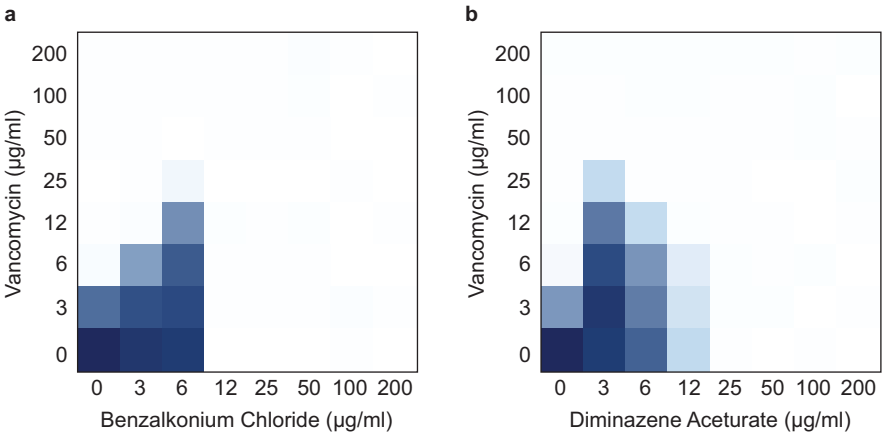

Supplementary Figure 1. Vancomycin suppression at 15°C by benzalkonium chloride and diminazene aceturate. a, Checkerboard broth microdilution assay showing dose-dependent vancomycin suppression by benzalkonium chloride against wild type *E. coli* grown at 15°C. Dark regions represent higher cell density. **b,** Same as in **a**, except cells were treated with diminazene aceturate. Note that pentamidine displays the strongest suppression of vancomycin activity relative to benzalkonium chloride or diminazene aceturate.

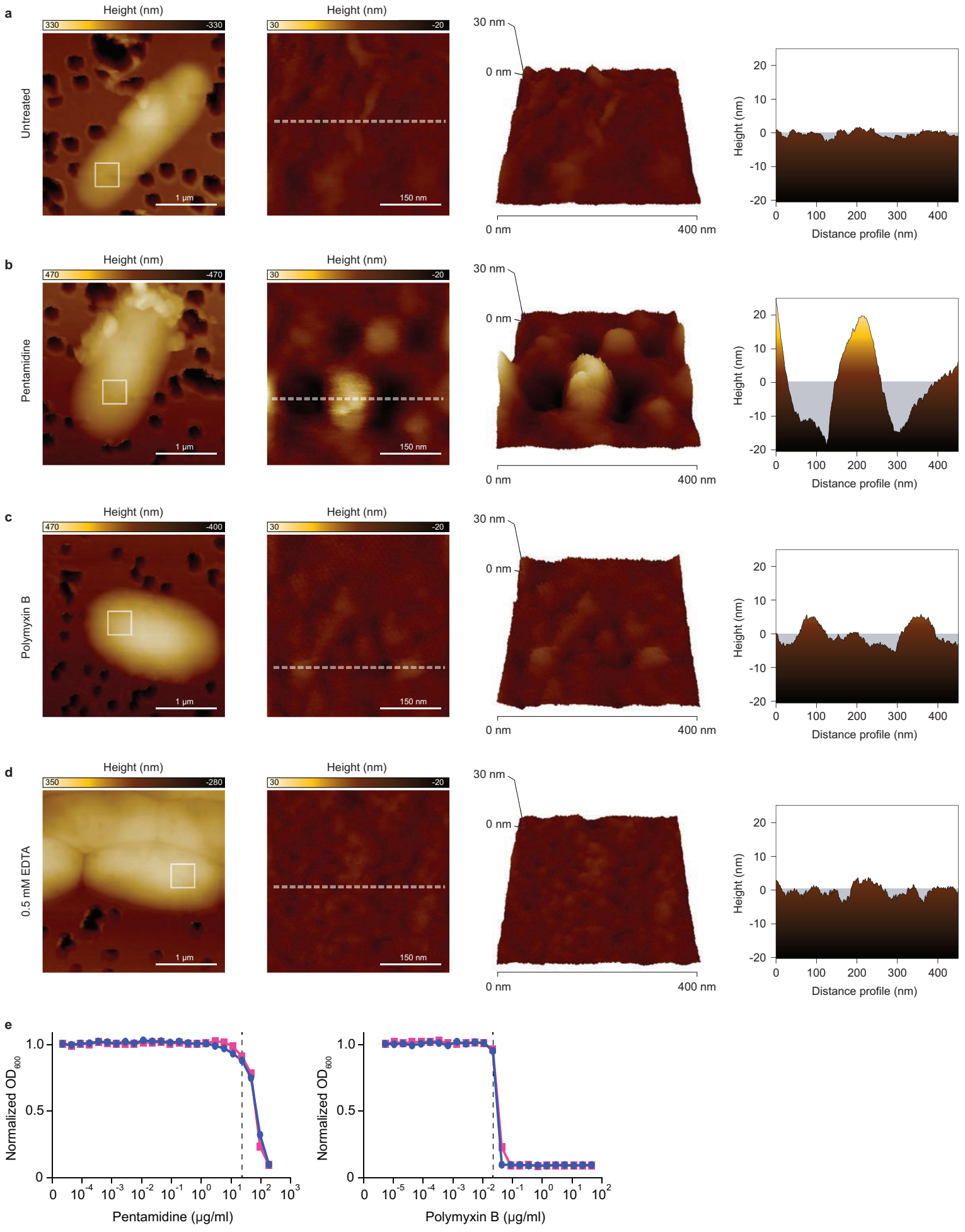
a
Untreated
Height (nm)
330
-330
1 µm
Height (nm)
30
-20
150 nm
30 nm
0 nm
0 nm
400 nm
Height (nm)
Distance profile (nm)
b
Pentamidine
Height (nm)
470
-470
1 µm
Height (nm)
30
-20
150 nm
30 nm
0 nm
0 nm
400 nm
Height (nm)
Distance profile (nm)
c
Polymyxin B
Height (nm)
470
-400
1 µm
Height (nm)
30
-20
150 nm
30 nm
0 nm
0 nm
400 nm
Height (nm)
Distance profile (nm)
d
0.5 mM EDTA
Height (nm)
350
-280
1 µm
Height (nm)
30
-20
150 nm
30 nm
0 nm
0 nm
400 nm
Height (nm)
Distance profile (nm)
e
Normalized OD600
Pentamidine (µg/ml)
Normalized OD600
Polymyxin B (µg/ml)

Supplementary Figure 2. Cell surface analyses of *E. coli* treated with outer membrane-active molecules. a, Atomic force micrographs of wild type *E. coli* grown in LB at 37°C to mid-log phase (OD~0.5). The white box (far left) highlights the region scanned to obtain high-resolution topographical images of the cell surface (right). The dotted line highlights the cross section used to generate two-dimensional height profiles (far right). Scans were acquired at 25°C, with scan rates of 0.5 Hz and 512 samples per line resolution. Height images were flattened to compensate for cell curvature, and topographical sections were used to generate 2-dimensional and 3-dimensional reconstructions of surface texture. **b,** Atomic force micrographs of wild type *E. coli* grown to mid-log phase in LB supplemented with pentamidine were acquired as in **a**. **c,** Atomic force micrographs of wild type *E. coli* grown to mid-log phase in LB supplemented with polymyxin B were acquired as in **a**. **d,** Atomic force micrographs of wild type *E. coli* grown to mid-log phase in LB supplemented with 0.5 mM EDTA were acquired as in **a**. **e,** Potency analyses of pentamidine (left) and polymyxin B (right) against wild type *E. coli* grown at 37°C in biological duplicate (pink and blue). Hashed lines represent the concentrations of each molecule that were used for the acquisition of atomic force micrographs.

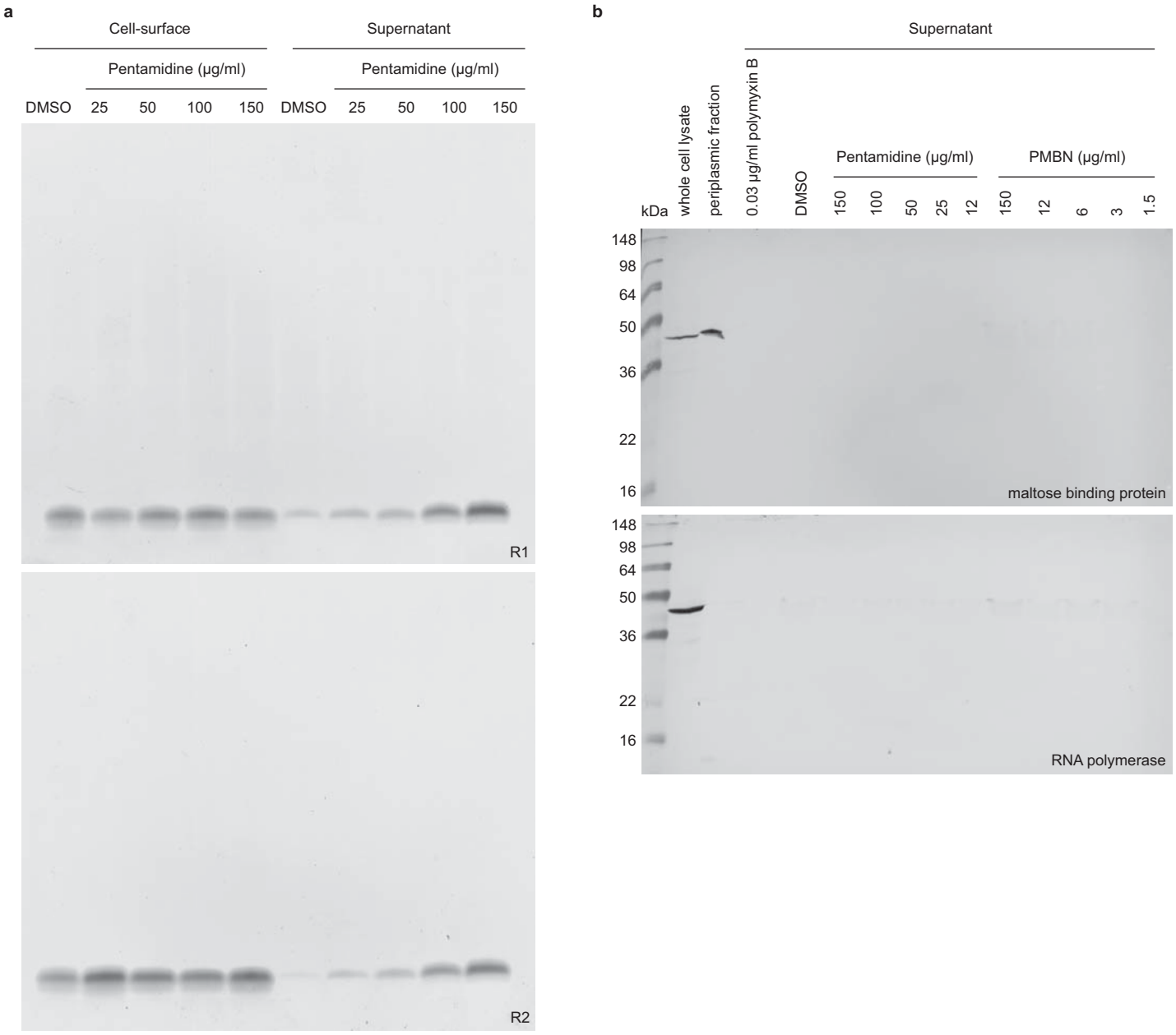

Supplementary Figure 3. Pentamidine-dependent perturbation of the outer membrane in *E. coli*. a, Cell-associated core OS (left), and core OS released into the growth medium (right), from wild type *E. coli* grown in the presence of pentamidine. Cells were grown at 37°C until mid-log phase (OD~0.5) in duplicate (top and bottom). **b,** Drug-induced leakage of periplasmic maltose binding protein (top) and cytoplasmic RNA polymerase (bottom). Wild type *E. coli* was grown at 37°C until mid-log phase (OD~0.5) in the presence of pentamidine, PMBN, or sub-inhibitory polymyxin B, and culture supernatants were subject to SDS-PAGE followed by Western blotting. Note that cells were treated with the same concentration of polymyxin B that was used for atomic force microscopy (Supplementary Fig. 2).

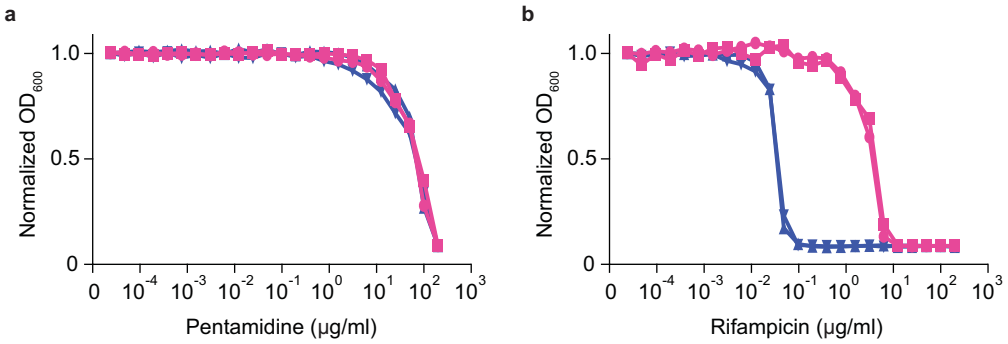

Supplementary Figure 4. Sensitivity of wild type and Δ*waaC E. coli* to pentamidine and rifampicin. a, Potency analyses of pentamidine against wild type *E. coli* (pink), and Δ*waaC E. coli* displaying deep rough LPS (blue). Cells were grown at 37°C in biological duplicate. **b,** Potency analyses of rifampicin against wild type *E. coli* (pink) and Δ *waaC E. coli* (blue). Cells were grown at 37°C in biological duplicate. Note that the activity of pentamidine alone is not enhanced in cells with increased outer membrane permeability.

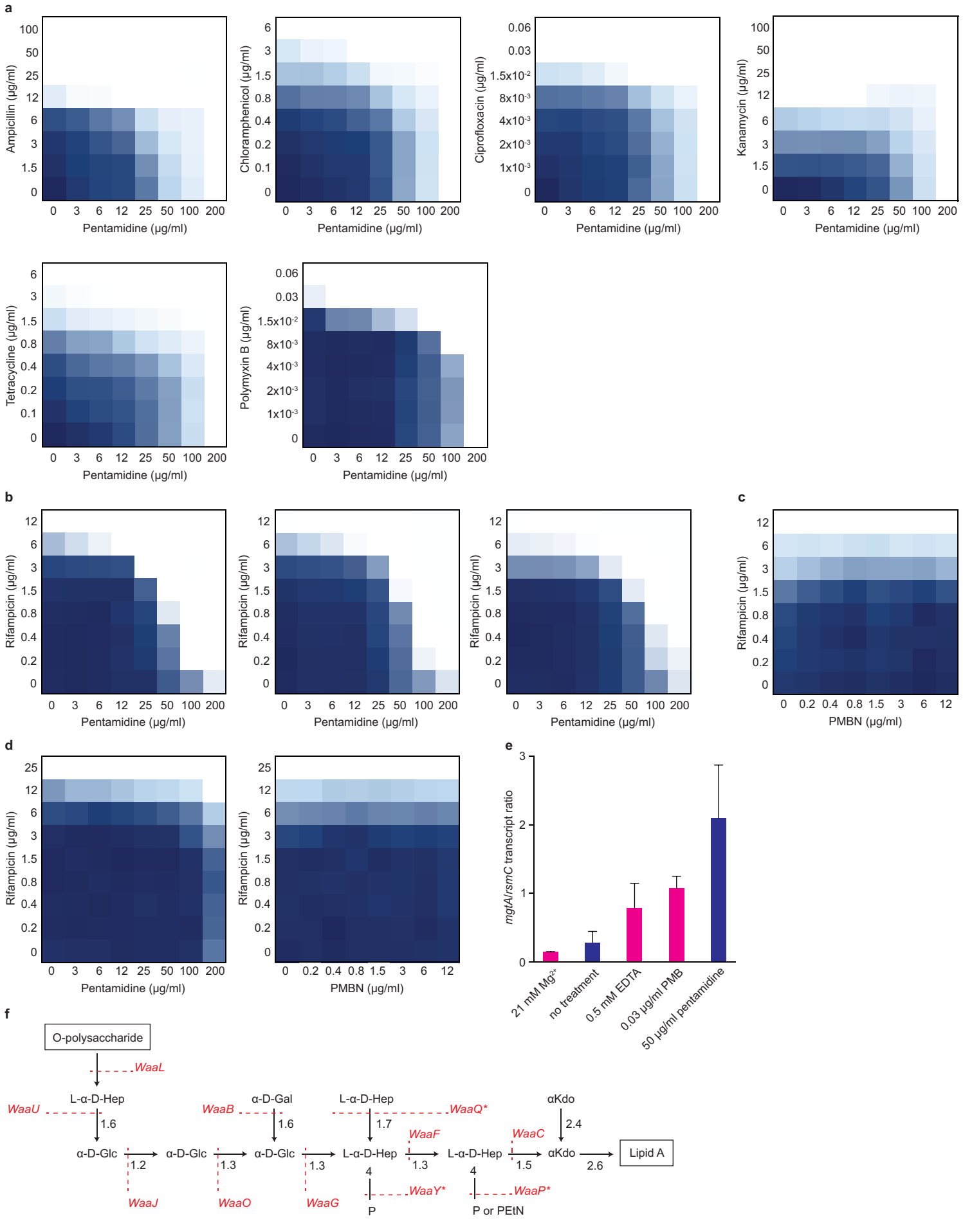
a
Ampicillin (μg/ml)
Chloramphenicol (μg/ml)
Ciprofloxacin (μg/ml)
Kanamycin (μg/ml)
Tetracycline (μg/ml)
Polymyxin B (μg/ml)
Pentamidine (μg/ml)
b
Rifampicin (μg/ml)
Pentamidine (μg/ml)
c
Rifampicin (μg/ml)
PMBN (μg/ml)
d
Rifampicin (μg/ml)
Pentamidine (μg/ml)
PMBN (μg/ml)
e
mgtA/rsmC transcript ratio
21 mM Mg2+
no treatment
0.5 mM EDTA
0.03 μg/ml PMB
50 μg/ml pentamidine
f
O-polysaccharide
WaaL
WaaU
L-α-D-Hep
1.6
α-D-Glc
1.2
WaaJ
α-D-Glc
WaaB
α-D-Gal
1.6
1.3
WaaO
α-D-Glc
1.3
WaaG
L-α-D-Hep
1.7
WaaQ*
4
WaaY*
P
WaaF
L-α-D-Hep
1.3
4
WaaP*
P or PEtN
WaaC
αKdo
2.4
1.5
αKdo
2.6
Lipid A

Supplementary Figure 5. Pentamidine-dependent potentiation of antibiotics against *E. coli*. a, Checkerboard broth microdilution assays between pentamidine and various structural classes of Gram-negative active antibiotics against wild type *E. coli* at 37°C. Dark regions represent higher cell density. **b,** Purified *E. coli* LPS was added to growth medium, and wild type *E. coli* was grown in the presence of varying concentrations of pentamidine and rifampicin at 37°C. LPS was added to final concentrations of 0.25 mg/ml (left), 0.5 mg/ml (middle), and 1 mg/ml (right). Dark regions represent higher cell density. **c,** Purified *E. coli* LPS (2 mg/ml) was added to growth medium, and wild type *E. coli* was grown in the presence of varying concentrations of PMBN and rifampicin at 37°C. Dark regions represent higher cell density. **d,** Checkerboard broth microdilution assays between pentamidine and rifampicin (left) or PMBN and rifampicin (right) against wild type *E. coli* in LB media supplemented with 21 mM Mg^{2+}. Cells were grown at 37°C. Dark regions represent higher cell density. **e,** Suppression or activation of the PhoPQ two-component system by Mg^{2+}, EDTA, and polymyxin B (PMB). Wild type *E. coli* was grown at 37°C until mid-log phase (OD~0.5), and transcript levels of the PhoPQ-dependent gene *mgtA*[42] were quantified relative to the housekeeping gene *rsmC* using quantitative reverse transcription PCR. Data are the means with standard error from two biological replicates. **f,** Structure of wild type *E. coli* core OS and genes involved in its biosynthesis. Asterisks highlight biosynthetic genes that are functionally interdependent. Note that *E. coli* BW25113 does not contain O-polysaccharide.

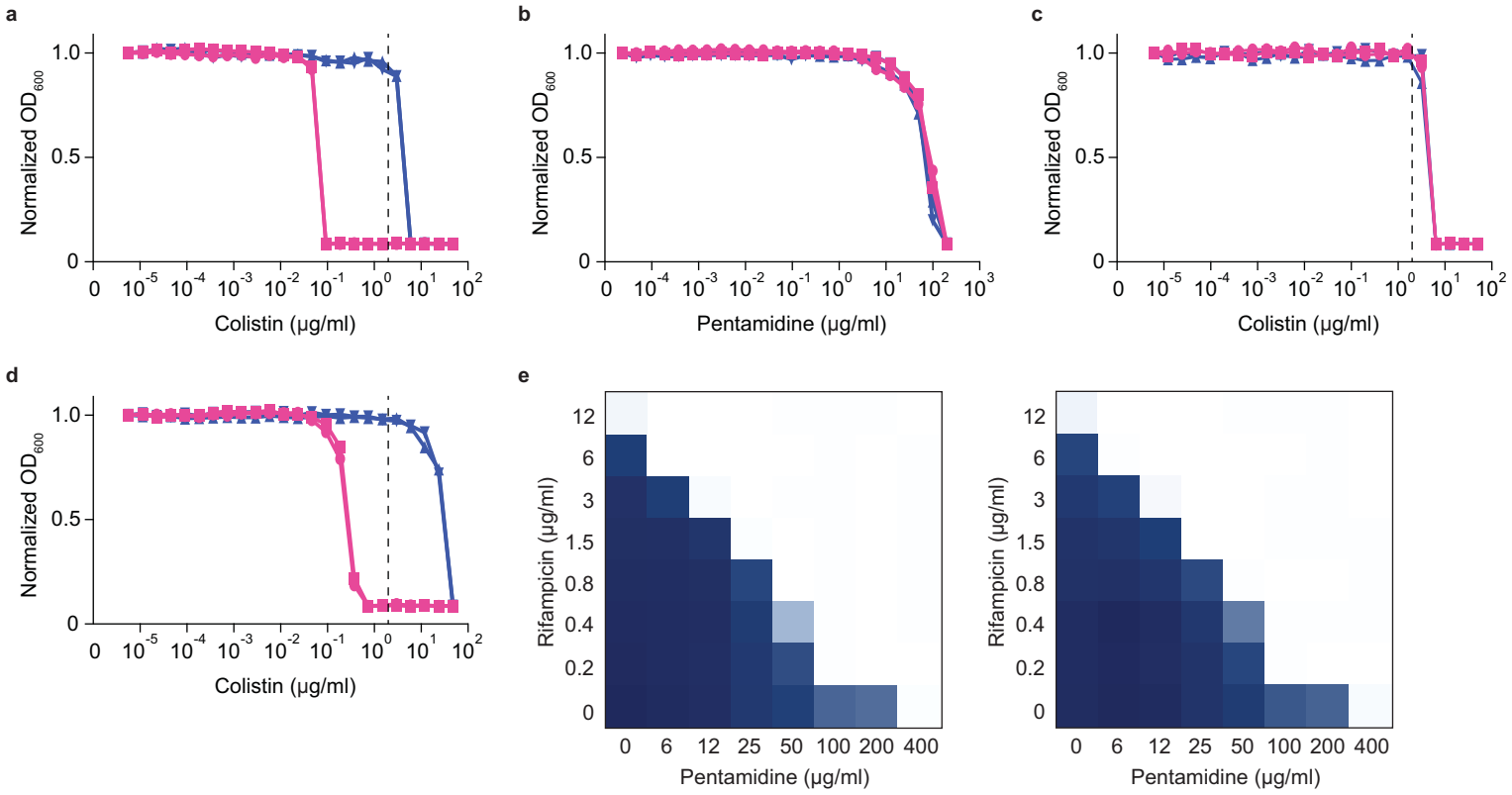

Supplementary Figure 6. Sensitivity of *mcr-1* positive *E. coli* and *K. pneumoniae* to colistin and pentamidine. **a,** Potency analyses of colistin against wild type *E. coli* (pink) and *E. coli* expressing *mcr-1* from the pGDP2 plasmid (blue). Cells were grown at 37°C in biological duplicate. **b,** Potency analyses of pentamidine against wild type *E. coli* (pink) and *E. coli* expressing *mcr-1* from the pGDP2 plasmid (blue). Cells were grown at 37°C in biological duplicate. **c,** Potency analyses of colistin against *E. coli* isolate N15-02865 (pink) and N15-02866 (blue). Cells were grown at 37°C in biological duplicate. **d,** Potency analyses of colistin against wild type *K. pneumoniae* (pink) and *K. pneumoniae* expressing *mcr-1* from the pGDP2 plasmid (blue). Cells were grown at 37°C in biological duplicate. Hashed lines represent the clinical MIC breakpoint for colistin (2 μg/ml). **e,** Checkerboard broth microdilution assays showing dose-dependent rifampicin potentiation by pentamidine against wild type *K. pneumoniae* (left) and *K. pneumoniae* expressing the *mcr-1* gene from the pGDP2 plasmid (right) at 37°C. Dark regions represent higher cell density.

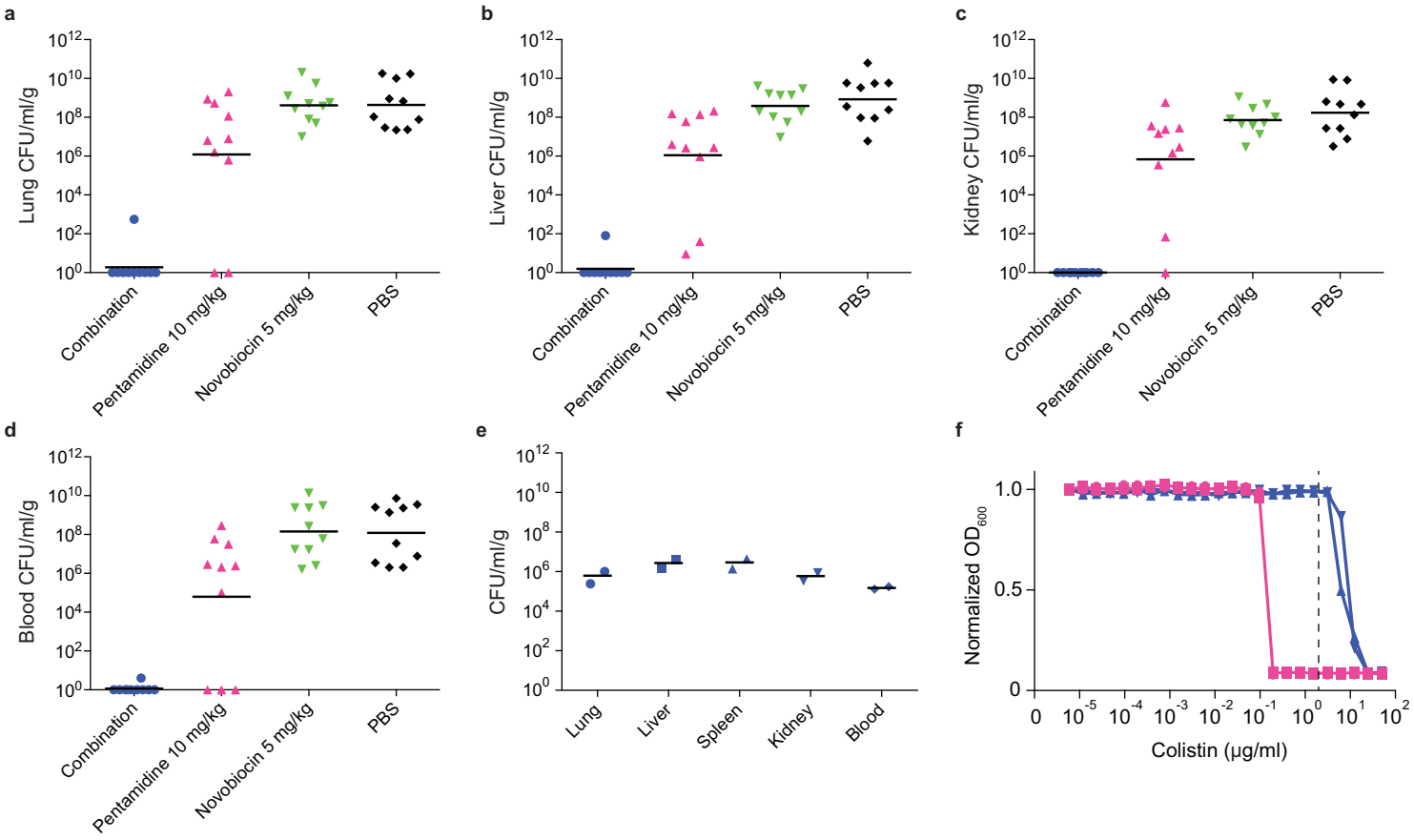

Supplementary Figure 7. *In vivo* efficacy of pentamidine against colistin-sensitive and -resistant *A. baumannii*. Bacterial loads of colistin sensitive *A. baumannii* ATCC 17978 in the lung **(a)**, liver **(b)**, kidney **(c)**, and blood **(d)** at phenotypic or experimental endpoint were determined by selective plating on chloramphenicol. Black lines represent geometric mean of the bacterial load for each treatment group. **e,** Bacterial loads of colistin sensitive *A. baumannii* ATCC 17978 in various organ tissues at 2-hours post infection with ~2x10^6 CFU injected intraperitoneally (n=2). Note that all organs harvested contained ~10^6 CFU/ml/g, showing full organ occupancy at time of initial treatment. **f,** Potency analyses of colistin against colistin sensitive *A. baumannii* ATCC 17978 (pink) and the colistin resistant variant of *A. baumannii* ATCC 17978 (blue). Cells were grown at 37°C in duplicate. Hashed line represents the clinical MIC breakpoint for colistin (2 µg/ml).